Journal of Cardiology (2009) 53, 265—271

ELSEVIER

CARDIOLOGY
Official Journal of the Japanese College of Cardiology

www.elsevier.com/locate/jjcc

ORIGINAL ARTICLE

Practical assessment of myocardial viability with a positron coincidence gamma camera using ^{18}F-fluorodeoxyglucose in acute myocardial infarction: Comparison with dedicated positron emission tomography and ^{201}Tl single photon emission computed tomography

Ryotaro Seki (MD)*, Hidenori Seki (MD), Takuji Toyama (MD, FJCC), Keiko Koyama (MD), Keigo Endo (MD), Masahiko Kurabayashi (MD, FJCC)

Department of Medicine and Biological Science, Graduate School of Medical Sciences, Gunma University, 3-39-15 Showamachi, Gunma-pref., Maebashi 371-8511, Japan

Received 14 October 2008; received in revised form 13 November 2008; accepted 19 November 2008
Available online 5 March 2009

KEYWORDS
PCD;
Coincidence detection;
PET;
Myocardial infarction;
FDG;
Tl

Summary
Objective: 2-[^{18}F] fluoro-2-deoxy-D-glucose (^{18}F-FDG) began to be supplied commercially to our hospital, which does not have a cyclotron, in autumn of 2005. The purpose of this study was to compare the utility of a dual-head positron coincidence detection (PCD) gamma camera in the detection of myocardial viability using ^{18}F-FDG with that of dedicated positron emission tomography (PET) and with that of thalium-201 (^{201}Tl) single photon emission computed tomography (SPECT).
Methods: A total of 15 patients (14 men and 1 woman, mean age: 60 ± 7 years, range: 46—73) with a large acute myocardial infarction (AMI) underwent ^{18}F-FDG PET, ^{18}F-FDG PCD imaging after oral glucose loading (75 g) and ^{201}Tl SPECT imaging. We divided the SPECT and PET images into a total of 20 segments, and semiquantitative visual analysis was performed by assessing regional tracer activities on a 4-point scoring system (DS): 0 = normal uptake, 1 = mildly reduced uptake, 2 = severely reduced uptake, and 3 = no uptake. We summed the DS in each patient as the total DS (TDS).
Results: The TDS of the ^{18}F-FDG PET image was 14.4 ± 7.7. The TDS of the ^{18}F-FDG PCD image was 18.7 ± 7.7. The TDS of the ^{201}Tl SPECT image was 24.1 ± 11.5. The

* Corresponding author. Tel.: +81 276 72 3140; fax: +81 276 72 5445.
E-mail address: sekiryo@d9.dion.ne.jp (R. Seki).

0914-5087/$ — see front matter
doi:10.1016/j.jjcc.2008.11.009

TDS of the ^{18}F-FDG PET image was significantly smaller than that of the ^{18}F-FDG PCD image. The TDS of the ^{18}F-FDG PET image was significantly smaller than that of the ^{201}Tl SPECT image. The TDS of the ^{18}F-FDG PCD image was significantly smaller than that of the ^{201}Tl SPECT image.
Conclusion: The findings of the project suggest that ^{18}F-FDG PCD is a good modality based on its accuracy, convenience, and cost-performance for detecting myocardial viability in hospitals that do not have a PET system.

Introduction

Positron emission tomography (PET) represents the most advanced scintigraphic imaging technique developed for in vivo evaluation of cardiac physiology and biochemistry. A large number of radiopharmaceuticals have been developed to study myocardial perfusion, energy metabolism, and autonomic innervation. Metabolic imaging with 2-[^{18}F] fluoro-2-deoxy-D-glucose (^{18}F-FDG) has emerged as an important clinical application for the assessment of tissue viability in patients with coronary artery disease (CAD) and impaired left ventricular function [1]. It is of great clinical value in determining if invasive revascularization therapy or conservative medical treatment should be instituted. PET imaging with FDG has been widely used to assess myocardial viability in patients with myocardial infarction because it provides accurate information concerning the differentiation of reversibly ischemic myocardium from scar tissue [2—6]. However, widespread implementation of PET as a clinical imaging modality has been hindered by the high cost of the imaging system, cyclotrons, support laboratories, maintenance, and operation [7]. Recently, ^{18}F-FDG imaging using single photon emission tomography (SPECT) with 511 keV collimators was introduced as an alternative method for the evaluation of myocardial metabolism and viability. However, discordance between SPECT and PET and the loss of accuracy for the detection of viable myocardium can occur due to the more limited spatial resolution and lower counting sensitivity compared with dedicated PET [8—11]. More recently, dual-head gamma cameras modified with positron coincidence detection (PCD) have become available for ^{18}F-FDG imaging, which provided comparable spatial resolution and system sensitivity as PET [12,13]. Although ^{18}F-FDG imaging using PCD has been validated and mainly used for tumor detection, the cardiac application of ^{18}F-FDG PCD imaging is still limited [14,15]. The purpose of this study was to investigate the potential ability of quantitative ^{18}F-FDG PCD to evaluate myocardial viability compared with a dedicated PET camera using ^{18}F-FDG.

Materials and methods

Imaging instrument

^{18}F-FDG PCD imaging was performed using a gamma camera equipped with 19-mm thick NaI (Tl) crystals and rectangular field of view detectors with a field of view of 50 cm × 30 cm (PCD, Picker New York City, NY, USA). Two detectors were positioned opposite each other with the capability of simultaneously detecting one annihilation photon in each detector resulting from the same positron emitter. A 15-ns timing window was applied to identify coincidence events. Additionally, a dual-window technique was used to accept the coincidences between photopeak—photopeak events and photopeak—Compton scatter events. Slit collimators were used to reduce the accidental coincidence counts from activity outside the field of view and reduce the effects of low-energy scattered radiation in the two-dimensional acquisition mode. The pre-windows were adjusted to 511 keV ± 30% of photopeak and the physical measurements of PCD for the spatial resolution, system sensitivity, count rate, and scatter fraction are reported in Table 1. ^{18}F-FDG PET imaging was performed with a dedicated PET (SET-2400W, Shimadzu, Kyoto, Japan), which had a large 20-cm axial field of view and a 59.5-cm transaxial field of view, and consisted of 32 rings of 21504 BGO crystals, giving 63 two-dimensional imaging planes. Signals from the photomultiplier tubes were processed to the position of the crystal in which the gamma photon hits it by using a coincidence time window of 15 ns. Position non-linearity and energy non-uniformity of the detector unit were corrected in real time. In the 2D mode, axial coincidence path acceptance was controlled from 1 to 8 to optimize sensitivity and axial resolution. The system had content septa 1-mm thick and 55-mm long for the 2D mode. Sixty-three sinograms

Table 1 Performance of the gamma camera and dedicated PET camera in two-dimensional mode.

Cameras	Resolution (FWHM:mm)	Sensitivity (kcps per kBq ml^{-1})	Scatter function (%)	NERC	
				kcps	kBq ml^{-1}
PET	4.4	8	13.1	73	28
PCD	5.7	1.8	22	3.9	0.2

PCD, coincidence gamma camera; PET, SET-2400W; NECR, noise-equivalent count rate.

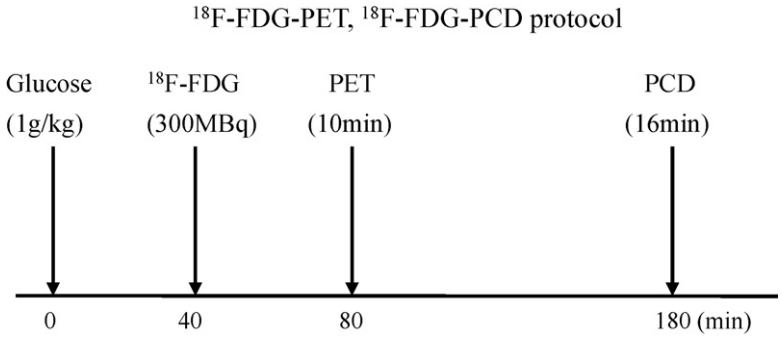

Figure 1 ^{18}F-FDG imaging protocol. FDG (300 MBq) was injected intravenously after 75 g oral glucose loading, and ^{18}F-FDG PET and ^{18}F-FDG PCD imaging was performed after 50 min and 110 min, respectively.

were stored in a large acquisition memory (1 GB) in the 2D mode. A dead time correction and physical decay correction of radioisotope were performed in real time in the memory. A ^{68}Ge—^{68}Ga transmission scan using a 185 MBq external rod source was acquired in a 640 mm radius. A simultaneous transmission—emission scan was performed in the SET-2400W PET. The protocol for PCD and PET is summarized in Fig. 1.

Patients

We recruited 15 patients (14 men and 1 woman, mean age: 60 ± 7 years, range: 46—73) with a large acute myocardial infarction (AMI) between May 2000 and April 2001. All patients underwent successful percutaneous intervention (PCI). Patients with restenosis, multiple-vessel disease, recent myocardial infarction (<6 weeks), unstable angina, diabetes, or concomitant heart disease (e.g. cardiomyopathy and valvular disease) were excluded. Patients with left bundle branch block, atrial fibrillation, or a permanent pacemaker were also excluded, since these factors would influence quantitative assessment of regional wall motion (Table 2). The involved vessel was the left anterior descending coronary artery in 12 patients, the left circumflex coronary artery in 2 patients, and the right coronary artery in 1 patient. The peak serum creatine kinase (CK) activity was 7593 ± 2818 IU ml^{-1} (range: 4151—11840), indicative of a large infarction. A value for the CK exceeding 4000 IU ml^{-1} was used to select patients having a large infarction. The mean time from onset of infarction to reperfusion was 5 ± 6 h (range: 30 min—19 h). Coronary stents were implanted in all patients, including MULTI-LINK stents in two cases, a GFX stent in one case, and NIR stents in eight cases. One patient required two coronary stents. Intra-aortic balloon pumping (IABP) was used in four cases after PCI. All patients were appropriately informed according to the Regulations and Guidelines for Research in the University and consented to participate in this study (Table 2).

Table 2 Patients' characteristics.

Age (years)	60 ± 7
Gender (men/women)	14/1
Vessel (LAD/LCX/RCA)	12/2/1
Peak CPK (IU ml^{-1})	7593 ± 2818
Mean time to reperfusion (h)	5 ± 6
Stent (multi-link/GFX/NIR)	2/1/8

LAD, left anterior descending coronary artery; LCX, left circumflex coronary artery; RCA, right coronary artery.

^{18}F-FDG PET imaging

Each patient was studied after an overnight fast and oral administration of a dose of 75 g of glucose 40 min before intravenous injection of approximately 300 MBq ^{18}F-FDG. Forty minutes later, a simultaneous transmission—emission

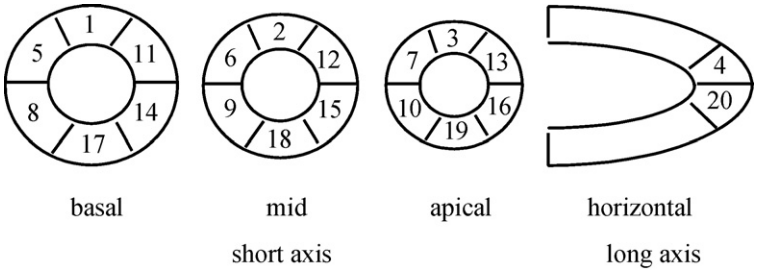

Figure 2 Diagrammatic indication of 20 segments used for the myocardial viability study in SPECT and PET; one vertical long-axis slice and three short-axis views at apical, middle, and basal ventricular levels. Semiquantitative visual analysis was performed by assessing regional tracer activities on a 4-point scoring system (DS): 0 = normal uptake, 1 = mildly reduced uptake, 2 = severely reduced uptake, and 3 = no uptake.

scan was performed using 2D PET for 10 min per bed position. The ordered subsets expectation maximization (OSEM) algorithm was used to reconstruct transaxial images with measured attenuation correction. The OSEM algorithm with 16 subsets and one iteration was used for 2D image reconstruction. The images produced using a Butterworth filter with a cut-off of 12 and order 2 were reconstructed to a 128×128 matrices. Decay and dead time correction were automatically performed during the acquisition step.

^{18}F-FDG PCD imaging

Cardiac images with PCD were obtained 98—109 min after the completion of ^{18}F-FDG PET, which was due to the count rate limitation of PCD (single count rate, approximately 1.1 cps). In all patients the heart was centered in the field of view to obtain optimal count sensitivity as well as axial and transverse resolution by giving the bed a right-sided offset. Prior to the start of acquisition, pulse height analysis revealed the absence of pulse pile-up in all patients. PCD data were acquired with a 180° rotation with 32 steps 30 s per step for a total of 16 min at one bed position. Decay and dead time correction were performed before image reconstruction. The emission data were corrected by uniform attenuation correction using Chang's method. The OSEM algorithm with the number of subsets equal to 32, iterations equal to 1, was used for 2D image reconstruction. The data were rebinned into 96 projections and images were reconstructed to a 128×128 matrices with a Butterworth filter (cut-off: 12, order: 2).

^{201}Tl imaging

Each patient received 111 MBq of ^{201}Tl. Fifteen minutes after the ^{201}Tl injection, patients underwent SPECT myocardial imaging. Myocardial SPECT imaging was performed using a PRISM 3000 (Picker) 3-headed SPECT system with low-energy, high-resolution, parallel-hole collimators. The detector system was interfaced to a dedicated nuclear medicine computer. A total of 60 projection images were obtained over 360° in 6° increments, with 40 s/view for ^{201}Tl. The energy discriminator was centered on 72 keV for ^{201}Tl with a 30% window. The data were recorded in 128×128 matrices on a magnetic disk. To reconstruct the transaxial tomographic images from each acquisition, Butterworth and ramp filters were used. The parameter of the Butterworth filter was >8, and the cutoff frequency was 0.15—0.17 cycle/pixel. Short- and long-axis slices (3.2-mm thick) also were generated. Subsequently, 3 serial slices (9.6-mm thick) SPECT images were generated.

Defect score

SPECT and PET defect scores were based on one vertical long-axis slice and three short-axis slices for each patient. In each patient, the corresponding vertical long- and short-axis tomograms from the ^{18}F-FDG PET, ^{18}F-FDG PCD, and ^{201}Tl SPECT image sets were aligned. Additionally, one vertical long-axis slice and three short-axis views at apical, middle, and basal ventricular levels were chosen for comparison. The vertical long-axis slice was used to evaluate the apical region, which was divided into two segments. Each short-axis slice was divided into six segments. The SPECT and PET images were therefore divided into a total of 20 segments (Fig. 2). All PET and SPECT images were displayed and analyzed by two experienced observers who were unaware of the patient's clinical history. Semiquantitative visual analysis was performed by assessing regional tracer activities on a 4-point scoring system (DS): 0 = normal uptake, 1 = mildly reduced uptake, 2 = severely reduced

Table 3 The comparison of ^{18}F-FDG PET and ^{18}F-FDG PCD images. In 226 of the 300 segments (all segments), the defect score corresponded between ^{18}F-FDG PET and ^{18}F-FDG PCD images (75%). In 69 of 143 abnormal uptake segments (=300 − 157) the defect score corresponded between ^{18}F-FDG PET and ^{18}F-FDG PCD images (48%).

	PCD 0	PCD 1	PCD 2	PCD 3	Total
PET 0	(157)	14	8	1	180
PET 1	5	16	14	6	41
PET 2	0	7	37	18	62
PET 3	0	0	1	16	17
Total	162	37	60	41	300

uptake, and 3 = no uptake. Disagreements in interpretation were resolved by consensus. We defined the sum of the DS in each patient as the total DS (TDS).

Results

Fifteen patients who underwent ^{18}F-FDG PET, ^{18}F-FDG PCD, and ^{201}Tl SPECT were evaluated in this study. A total of 300 segments in 15 patients were analyzed to evaluate the defect score from ^{18}F-FDG PET, ^{18}F-FDG PCD, and ^{201}Tl SPECT images. We assessed the defect score in all segments (300 segments), and moreover in abnormal uptake segments with myocardial damage due to AMI (defect score 1—3).

Table 4 The comparison of ^{18}F-FDG PET and ^{201}Tl SPECT images. In 161 of the 300 segments (all segments), the defect score corresponded between ^{18}F-FDG PET and ^{201}Tl SPECT images (54%). In 32 of 171 abnormal uptake segments (=300 − 129) the defect score corresponded between ^{18}F-FDG PET and ^{201}Tl SPECT images (19%).

	TL 0	TL 1	TL 2	TL 3	Total
PET 0	(129)	14	18	19	180
PET 1	7	7	13	9	41
PET 2	6	12	12	32	62
PET 3	0	0	4	13	17
Total	142	33	47	78	300

Table 5 The comparison of ^{18}F-FDG PCD and ^{201}Tl SPECT images. In 178 of the 300 segments (all segments), the defect score corresponded between ^{18}F-FDG PCD and ^{201}Tl SPECT images (59%). In 53 of 175 abnormal uptake segments (=300 − 125) the defect score corresponded between ^{18}F-FDG PCD and ^{201}Tl SPECT images (30%).

	TL 0	TL 1	TL 2	TL 3	Total
PCD 0	(125)	11	14	12	162
PCD 1	9	7	12	9	37
PCD 2	7	10	16	7	60
PCD 3	1	5	5	30	41
Total	142	33	47	78	300

The comparison of ^{18}F-FDG PET and ^{18}F-FDG PCD images

The overall agreement rate in regional ^{18}F-FDG defect score for all segments between ^{18}F-FDG PET and ^{18}F-FDG PCD images was 75% (226 of the 300 segments) (Table 3). In 69 of 143 abnormal uptake segments (=300 − 157) the defect score corresponded between ^{18}F-FDG PET and ^{18}F-FDG PCD images (48%) (Table 3).

The comparison of ^{18}F-FDG PET and ^{201}Tl SPECT images

The overall agreement rate in regional defect score for all segments between ^{18}F-FDG PET and ^{201}Tl SPECT images was 54% (161 of the 300 segments) (Table 4). In 32 of 171 abnormal uptake segments (=300 − 129) the defect score corresponded

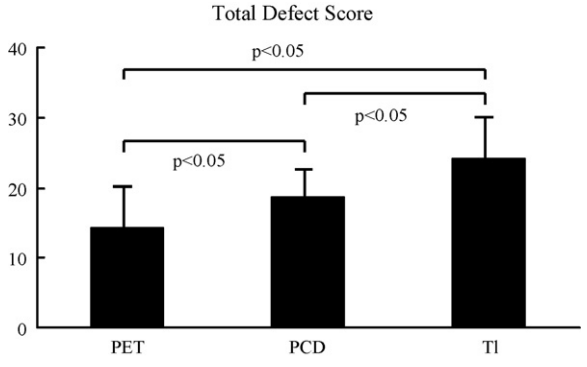

Figure 3 The TDS of the ^{18}F-FDG PET image was 14.4 ± 7.7. The TDS of the ^{18}F-FDG PCD image was 18.7 ± 7.7. The TDS of the ^{201}Tl SPECT image was 24.1 ± 11.5.

between ^{18}F-FDG PET and ^{201}Tl SPECT images (19%) (Table 4).

The comparison of ^{18}F-FDG PCD and ^{201}Tl SPECT images

The overall agreement rate in regional defect score for all segments between ^{18}F-FDG PCD and ^{201}Tl SPECT images was 59% (178 of the 300 segments) (Table 5). In 53 of 175 abnormal uptake segments (=300 − 125) the defect score corresponded between ^{18}F-FDG PCD and ^{201}Tl SPECT images (30%) (Table 5).

Total defect score

These defect scores were summed to yield TDS for each image. The TDS of the ^{18}F-FDG PET image was 14.4 ± 7.7. The TDS of the ^{18}F-FDG PCD image was 18.7 ± 7.7. The TDS of the ^{201}Tl SPECT image was 24.1 ± 11.5. The TDS of the ^{18}F-FDG PET image was significantly smaller than that of the ^{18}F-FDG PCD image. The TDS of the ^{18}F-FDG PET image was significantly smaller than that of the ^{201}Tl SPECT image. The TDS of the ^{18}F-FDG PCD image was significantly smaller than that of the ^{201}Tl SPECT image (Fig. 3).

Discussion

The assessment of myocardial viability has an important role in the diagnostic and prognostic evaluation after an acute myocardial infarction. Various techniques have been reported to identify the viable myocardium, such as SPECT with ^{201}Tl or ^{99m}Tc sestamibi, ^{18}F-FDG PET, combination of dual tracers (e.g. ^{131}I-BMIPP SPECT and ^{99m}Tc-TF SPECT), and dobutamine stressed echocardiography. ^{201}Tl SPECT has been established as a clinically important method to assess perfusion and sarcolammal integrity, and hence to assess myocardial viability. Many studies have compared ^{99m}Tc sestamibi SPECT with ^{18}F-FDG imaging. The majority of these studies have shown that ^{18}F-FDG imaging is more sensitive than ^{99m}Tc sestamibi SPECT for the detection of viable myocardium. Several investigators have suggested that attenuation may be responsible for this phenomenon because underestimation of viability by ^{99m}Tc sestamibi occurs predominantly in the inferior wall. ^{18}F-FDG PET is considered the non-invasive 'gold standard' for identifying viable myocardium. However, widespread application has been hampered by the relatively high cost and limited availability of the technique. Consequently, substantial effort has been invested in the development of high-energy SPECT imaging using 511-keV collimators. The major disadvantages of the approach are its low resolution and low counting sensitivity. Coincidence imaging using a parallel, dual-head gamma camera was introduced to overcome these limitations. In recent years, much effort has been devoted to comparing the feasibility and efficiency between coincidence gamma cameras and dedicated PET in the field of oncology. Additionally, there have been attempts to apply the theoretic potential advantages of coincidence gamma cameras to nuclear cardiology. Nevertheless, data on cardiac metabolic imaging after revascularization therapy in AMI using ^{18}F-FDG are still limited.

In this study, we evaluated myocardial viability using ^{18}F-FDG PET, ^{18}F-FDG PCD, and ^{201}Tl SPECT. ^{18}F-FDG uptake is known to differ depending on the dietary condition. ^{18}F-FDG imaging in the fasting state provides a sensitive signal for identifying myocardial regions with reduced oxygen supply, as reflected by the compensatory shift toward greater glucose utilization to generate high-energy phosphates (hibernating but viable myocardium). In an overnight fasting condition, ^{18}F-FDG uptake may overestimate the viable tissue. Lack of ^{18}F-FDG signal in the fasting state, however, may represent either normal myocardium or scarred myocardium. In the glucose-loaded state, ^{18}F-FDG imaging identifies all metabolically viable myocardial regions, which include normal, hibernating, and stunned myocardium [16]. For that reason, we administered a definite dose of glucose (75 g) to each patient after overnight fasting, and we estimated the myocardial viability compared with ^{18}F-FDG uptake in the healthy myocardium relatively. The TDS of ^{18}F-FDG PCD was significantly higher than that of ^{18}F-FDG PET. We expected there would be no significant difference between ^{18}F-FDG PCD and ^{18}F-FDG PET. Tian et al. reported that regional analysis showed a lower agreement between ^{18}F-FDG PCD and ^{18}F-FDG PET in the inferior and septal walls compared with the other walls [17]. A false positive for myocardial viability could be created by an overestimation of relative ^{18}F-FDG uptake in the anterior region, caused by the underestimation of ^{18}F-FDG uptake in the posterior—inferior region. Coronary angiography of the 15 patients showed the culprit vessel was the left anterior descending coronary artery in 12, the left circumflex coronary artery in 2, and the right coronary artery in 1. This vessel distribution does not explain the difference between ^{18}F-FDG PCD and ^{18}F-FDG PET. In this study, ^{18}F-FDG PCD and ^{18}F-FDG PET image acquisitions were started at different times

after ^{18}F-FDG administration. The different times of acquisition might be partly responsible for the different distribution in the myocardium or other organs and blood. Moreover, a higher percentage of scatter and randomness in ^{18}F-FDG PCD imaging has been reported [18], and pulse pile-up in the detector system limits the single count rate of PCD imaging. These factors may have resulted in lower concordance between ^{18}F-FDG PCD and ^{18}F-FDG PET. Another study reported comparable overall agreement (93%) between ^{18}F-FDG PCD and ^{18}F-FDG PET in evaluating myocardial viability using a quantitative method. In clinical use, myocardial perfusion imaging replaces ^{18}F-FDG PET to detect myocardial viability although many studies have reported that perfusion imaging can underestimate myocardial viability. In this study, the TDS of the ^{201}Tl SPECT image was significantly higher than that of the ^{18}F-FDG PET image. The TDS of the ^{18}F-FDG PCD image also was significantly lower than that of the TDS of ^{201}Tl SPECT. Using a gamma camera, ^{18}F-FDG PCD can detect myocardial viability more accurately than ^{201}Tl SPECT. In hospitals that do not have a PET system, ^{18}F-FDG PCD is a good modality based on its accuracy, convenience, and cost-performance for detecting myocardial viability.

References

[1] Topol EJ. Comprehensive cardiovascular medicine, vol. 2. Philadelphia: Lippincott-Raven; 1998. p. 1587—1613.

[2] Marshall RC, Tillisch JH, Phelps ME, Huang SC, Carson R, Henze E, Schelbert HR. Identification and differentiation of resting myocardial ischemia and infarction in man with positron computed tomography, ^{18}F-labeled fluorodeoxyglucose and N-13 ammonia. Circulation 1983;67:766—88.

[3] Schwaiger M, Brunken R, Grover-Mckay M, Krivokapich J, Child J, Tillisch JH, Phelps ME, Schelbert HR. Regional myocardial metabolism in patients with acute myocardial infarction assessed by positron emission tomography. J Am Coll Cardiol 1986;8:800—8.

[4] Brunken R, Tillisch J, Schwaiger M, Child JS, Marshall R, Mandelkern M, Phelps ME, Schelbert HR. Regional perfusion, glucose metabolism, and wall motion in patients with chronic electrocardiographic Q-wave infarctions: evidence for persistence of viable tissue in some infarct regions by positron emission tomography. Circulation 1986;73: 951—63.

[5] Altehoefer C, Kaise H-J, Dörr R, Feinendegen C, Beilin I, Uebis R, Buell U. Fluorine-18 deoxyglucose PET for assessment of viable myocardium in perfusion defects in ^{99m}Tc-MIBI SPET: a comparative study in patients with coronary artery disease. Eur J Nucl Med 1992;19: 334—42.

[6] Tamaki N, Kawamoto M, Tadamura E, Magata Y, Yonekura Y, Nohara R, Sasayama S, Nishimura K, Ban T, Konishi J. Prediction of reversible ischemia after revascularization: perfusion and metabolic studies with positron emission tomography. Circulation 1995;91:1697—705.

[7] Conti PS, Keppler JS, Halls JM. Positron emission tomography: a financial and operational analysis. Am J Roentgenol 1994;162:1279—86.

[8] Maddahi J, Schelbert H, Brunken R, Di Carlu M. Role of thallium-201 and PET imaging in evaluation of myocardial viability and management of patients with coronary artery disease and left ventricular dysfunction. J Nucl Med 1994;35:707—15.

[9] Sandler MP, Bax JJ, Patton JA, Visser FC, Martin WH, Wijins S. Fluorine-18-fluorodeoxyglucose cardiac imaging using a modified scintillation camera. J Nucl Med 1998;39:2035—43.

[10] Chen EQ, MacIntyre WJ, Go RT, Brunken RC, Saha GB, Wong CY, Neumann DR, Cook SA, Khandekar SP. Myocardial viability studies using fluorine-18-FDG SPET: a comparison with fluorine-18-FDG PET. J Nucl Med 1997;38:582—6.

[11] Srinivasan G, Kitsiou AN, Bachantach SL, Bartlett ML, Miller-Davis C, Dilsizian V. ^{18}F-fluorodeoxyglucose single photon emission computed tomography. Can it replace PET and thallium SPET for the assessment of myocardial viability? Circulation 1998;97:843—50.

[12] Muellehner G, Geagen M, Countryman P, Nellemann P. SPECT scanner with PET coincidence capability. J Nucl Med 1995;36(Suppl.):70P.

[13] Zhang H, Tian M, Oriuch N, Higuchi T, Tanada S, Endo K. Detection of lung cancer with positron coincidence gamma camera using fluorodeoxyglucose in comparison with dedicated PET. Br J Radiol 2002;75:409—16.

[14] Hasegawa S, Uehara T, Yamaguchi H, Fujino K, Kusuoka H, Hori M, Nishimura T. Validity of ^{18}F-fluorodeoxyglucose imaging with a dual-head coincidence gamma camera for detection of myocardial viability. J Nucl Med 1999;40:1884—92.

[15] De Sutter J, De Winter F, Van de Wiele C, De Bondt P, D'Asseler Y, Dierckx R. Cardiac fluorine-18 fluorodeoxyglucose imaging using a dual-head gamma camera with coincidence detection: a clinical pilot study. Eur J Nucl Med 2000;27:676—85.

[16] Dilsizian V, Bacharach SL, Khin MM, Smith ME. Fluorine-18-deoxyglucose SPECT and coincidence imaging for myocardial viability: clinical and technologic issue. J Nucl Cardiol 2001;8:75—88.

[17] Tian M, Koyama K, Zhang H, Oriuchi N, Higuchi T, Endo K. Assessment of myocardial viability with a position coincidence gamma camera using fluorodeoxyglucose in comparison with dedicated PET. Nucl Med Commun 2003;24:367—74.

[18] Zhang H, Inoue T, Tian M, Alyafei S, Oriuchi N, Khan N, Li S, Endo K. A basic study on lesion detectability for hot spot imaging of positron emitters by dedicated PET and positron coincidence gamma camera. Ann Nucl Med 2001;15: 301—6.